Physical models for packed bed: Sensible heat storage systems

A. Elouali, Tarik Kousksou, T. El Rhafiki, S. Hamdaoui, M. Mahdaoui, A. Allouhi, Youssef Zeraouli

Physical Models for Packed Bed: Sensible Heat Storage Systems

A. Eloulai[(a)], T. Kousksou[(b)], T. El Rhafiki[(a)], S. Hamdaoui[(c)], M. Mahdaoui[(c)], A. Allouhi[(d)],Y. Zeraouli[(b)]

[(a)]Ecole Nationale Supérieure d'Arts et Métiers, ENSAM Marjane II, BP – 4024 Meknès Ismailia, Maroc.

[(b)]UNIV PAU&PAYS ADOUR/E2S UPPA, Laboratoire des Sciences de l'Ingénieur Appliquées à la Mécanique et au Génie Electrique – Fédération IPRA, EA 4581, 64000, Pau, France.

[(c)]Equipe de Recherche en Transferts Thermiques & Energétique – UAE/E14FST Département de Physique FST, Université Abdelmalek Essaâdi Tanger – Maroc.

[(d)]Université Sisi Mohamed Ibn Abdelah, Ecole Supérieur de Technologie de Fès, Route d'Imouzze BP 2427, Maroc.

Abstract: In this article, we discuss different physical models to evaluate the thermal performance of packed bed for sensible heat storage with air as the heat transfer fluid (HTF). The mathematical equations are numerically solved by applying the finite volume method, and the derived results are corroborated by the existing experiments in the literature. Numerical simulations are performed with different solid storage materials and for various mass flow rates of HTF, porosity and solid material size. Detailed characteristics of the packed bed are discussed and various numerical results are presented. The applicability of pressure drop and the thermal optimization of the packed bed are also discussed.

Keywords: Sensible heat storage; Heat transfer; Packed bed; Numerical models

1- Introduction

Thermal Energy Storage Systems (TESS) are considered as a key tool for decarbonization since they can issues related to energy efficiency and process flexibility, improve utilization of renewable energy resources and thus reduce greenhouse gas emissions. The use of TES for thermal applications, such as space and water heating, cooling, air-conditioning heat sinks, has recently received much attention **[1-5].** Three kinds of TESS are available:

- Sensible heat storage (SHS), through which heat is stored by increasing the storage medium temperature **[2];**
- Latent Heat Storage (LHS), where heat is stored/delivered during the melting/freezing of Phase Change Material (PCM) **[3-4]**;
- Thermo-chemical Heat Storage (TCHS), where heat is stored using reversible chemical reactions **[5].**

SHS systems represents the easiest and the most economical form of thermal storage **[6-7]**. Sensible heat storage materials (solids or liquids) are not subject to any phase transition during the storage period. The most important problem with sensible liquid storage materials is that they involve large storage reservoirs for both hot and cold (HTF) and high-cost heat exchangers **[8-10**]. Important work has been performed on SHS systems using various solid materials such as rocks, concrete, metals, sand, ceramics, and bricks. Nevertheless, for any SHS system, storage and recuperation of thermal energy must be carried out efficiently to reach high capacity performances. For this, SHS systems have to satisfy a number of criteria: high energy density, reliable heat transfer between HTF and solid storage media, low cost, and reversibility through multiple charge and discharge cycles [9-10]. . For this purpose, it is important to examine such technologies to better apprehend and conceive efficient SHS and encourage their introduction in the markets.

In this paper various physical models are developed to investigate the thermal performance of packed bed filled with spherical solid material for solar air heating applications. The effects of different parameters such as the inlet velocity of HTF, the diameter of the spherical solid material and the porosity of the tank during the charging process were presented.

2- Physical models

The packed bed is in general an aleatory aggregation of a spherical solid material, each in physical contact with its neighbors and maintained fixed in a container as illustrated in **Fig.1**. During the charging mode, the hot air flows through the packed bed and heats the solid storage material. The HTF leaves the packed bed cooled. To extract the thermal energy from the storage material (discharge mode), the flow direction is inverted and the incoming cooled air is gradually heated along the bed (see **Fig.1**). The ideal charging /discharging process is accomplished when all the spherical capsules are at the same temperature of the HTF at the inlet of the packed bed.

A wide range of publications have described numerical models for sensible heat storage in packed beds **[11-14].** They are all based on the original analytical work by Schumann [**15**]. The Schumann model is an unsteady and one dimensional model which permits to predict the axial distribution of both the solid and heat transfer fluid temperatures. Martin **[16]** performed a study in which he partitioned the packed bed into two zones, one close to the wall with a high void fraction and the other one in the mid-bed region. Cross et al. **[17]** used the results due to Martin **[16]** for the temperature distribution. His results seem to be accurate for liquid working fluids and not as good for gases as working fluids. Using the method due to Martin **[16],** Beasley and Clark **[18]** pointed out that the calculation time is high when the proportion of the specific heat of the solid to the specific heat of the heat transfer fluid is higher. Handley and Heggs **[19]** employed an alternative version of Schumann's model by considering a thermal gradient in the solid particles with the implicit Crank–Nicholson method to solve the model equations using gas as a heat transfer fluid. Beasley and Clark **[18**] solved the same problem by considering the bed wall effect. Furnas **[20]** conducted experiments with steel spheres of diameters 1.85; 3.87 and 4.86 cm to identify the heat transfer coefficient between the heat transfer fluid (air) and solid. He identified some correlations for the film coefficient suggesting that the film coefficient is not affected by the diameter of the sphere. Gunn **[21]** discussed various investigations of the impact of radial and axial dispersion in the packed bed. Vortmeyer and Schaefer **[22]** have illustrated that the single-phase model can be deduced from the continuous solid-phase model. Based on their

findings, Vortmeyer and Adam **[23]** identified the effective axial thermal dispersion in the bed as a function of Reynolds' and Peclet's numbers. Persons et al. **[24]** used the numerical code TRANSYS to study the packed bed using Schumann's model, compared the numerical predictions with experimental results and found good agreement. Melanson and Dixon **[25]** carried out experimental measurements on packed beds of a small diameter ratio of bed to the diameter of particles and identify the effective thermal conductivity and the heat transfer coefficient close to the bed wall. Their results in agreement with the Furnas conclusions **[20]**, reveal that particle size has a negligible impact on these two parameters. Hollands et al. **[26]** experimentally determined the radial distribution of the heat transfer fluid velocity in the packed bed and studied the effect of the velocity on the thermal performance of the packed bed. Coutier and Faber **[27]** used Schumann's model to invetigate the thermal behaviour of the packed bed. Also they quantify the volumetric heat transfer coefficient between the heat transfer fluid (air) and solid material experimentally. The obtained results are very helpful to design the thermal storage bed with air as HTF. Raiz **[28]** presented an analytical solution for packed beds based on Schumann's model and the one dimensional single phase model. Sowell and Curry **[29]** investigated the packed bed by using Schumann's model with possible variations in the heat transfer fluid inlet temperature. The outlet heat transfer fluid temperature is calculated by the addition of the inlet temperature multiplied by a response factor. Littman et al. **[30]** determined experimentally the heat transfer coefficient coefficient between heat transfer fluid and the solid material for small Reynolds number from 2 to 100 and diametr solid particles from 0.495 to 2.0 mm. While Gupta et a. **[31]** used experimental results in order to propose expressions for the Nusselt number between the solid particle and the heat transfer fluid for Reynolds number from 10 to 10^4 .Maaliou and McCoy **[32]** proposed an economic method to optimize the thermal energy storage inisde the packed bed with spherical solid particles. The economic value of the thermal energy stored is maximized in terms of the capital and operational costs. The mathematical model used is capable to determine the thermal gradient inside the solid particles and the heat losses to the external environment.

The physical models of packed bed TES system can be divided into two main categories **[11-12].** When the temperature of the solid material and the temperature of the HTF can be assumed equal at any specific location, the packed bed is likened to a homogeneous medium and the *single-phase model* can be applied. According to Ismail and Stuginsky **[14]** this model is useful in analyzing packed beds with high thermal conductivity and high thermal capacity of the storage medium in comparison to HTF. If the hypothesis on two-phase equality of

temperature is accepted, the heat diffusion in the solid and the HTF have to be regarded independently **[33-40].** In this group one can identify three models which can represent the dynamic behavior of the packed bed, that is, *Schumann's model*, the *continuous solid phase model* and the *concentric dispersion models* or models which allow for thermal gradients inside the solid particles **[41-50].** The last model assumes that the temperature profile is symmetrical with respect to the center of the particles.

The principal purpose of this study is to provide a comparative analysis of four physical models for packed bed sensible heat storage systems. In the formulation of these physical models, whose details are shown below, it is assumed that the bed geometry is cylindrical with height *H* and diameter of *D* and charged with spherical solid particle of diameter d. There is no heat generation within the bed, no chemical reactions, the radial heat conduction and the radiation heat transfer mechanism inside the packed bed are considered to negligible, there are no heat losses to the ambient and finally no thermal gradient inside the solid particles except in the case of the last model namely the concentric dispersion model.

2.1 The single phase model (Model 1)

In a packed beds having a significant volumetric heat transfer (between HTF and solid materials) and/or charged with solid materials of high conductivity, the thermal resistance between the solid particles and the HTF becomes negligible. In such a case one energy equation based on the homogeneous temperature T_m is sufficient to describe the thermal behavior of the packed bed:

$$(\rho c)_m \frac{\partial T_m}{\partial t} + G c_f \frac{\partial T_m}{\partial x} = \frac{\partial}{\partial x}\left(k_m \frac{\partial T_m}{\partial x} \right) \qquad \textbf{(1)}$$

The heat capacity of the packed bed, $(\rho.c)_m$, is the sum of the solid particles and the HTF contribution:

$$(\rho.c)_m = \varepsilon \rho_f c_f + (1-\varepsilon)\rho_s c_s \qquad \textbf{(2)}$$

where ρ and c are, respectively, the density and the specific heat; G is the mass velocity of the HTF, k_m is the effective thermal conductivity of the bed and ε is the porosity of the tank.

The effective thermal conductivity k_m is calculated by using the following expression [**49-50**]:

$$k_m = k_s \left[1 - \frac{\varepsilon.\left(k_s - k_f^*\right)}{k_f^* + \varepsilon^{1/3}\left(k_s - k_f^*\right)} \right] \quad \textbf{(3)}$$

where k_s is the thermal conductivity of the solid material and k_f^* is the effective thermal conductivity of the HTF. The expression of k_f^* is the following [**49-50**]:

$$\frac{k_f^*}{k_f} = \varepsilon\left(1 + c_1.\left(\mathrm{Re}_p.\mathrm{Pr}_f\right)^{c_2}\right) \quad \textbf{(4)}$$

With $0.115 \le c_1 \le 0.167$ and $1 \le c_2 \le 1.25$

$$\mathrm{Re}_p = \frac{\rho_f u.\mathrm{d}}{\mu_f} \text{ and } \mathrm{Pr}_f = \frac{c_f \mu_f}{k_f}$$

where u is the mean heat-transfer fluid flow velocity and μ_f is the dynamic viscosity of the HTF.

2.2 Schumann's model (Model 2)

The Schumann's one dimensional model **[15]** can be deduced from the general equation of energy conservation. In this case, it is supposed that there is no heat conduction in the fluid. The heat exchange between the solid particles is assumed to be negligible. The energy equation of the packed bed can be expressed as:

- **For HTF:**

$$\varepsilon(\rho c)_f\left(\frac{\partial T_f}{\partial t} + u\frac{\partial T_f}{\partial x}\right) = U.A\left(T_s - T_f\right) \quad \textbf{(5)}$$

- **For solid material**

$$(1-\varepsilon).(\rho c)_s \frac{\partial T_s}{\partial t} = U.A\left(T_{HTF} - T_s\right) \quad \textbf{(6)}$$

where U is the heat-transfer coefficient between the HTF and the solid particle; A is the superficial particle area per unit bed volume. A can be determined by the following expression:

$$A = \frac{6(1-\varepsilon)}{d} \tag{7}$$

2.3 Continuous solid phase model (Model 3)

In this model, the solid is assumed to behave as a continuous medium and not as a medium composed of independent solid particles. It is also assumed that the heat transfer in the bed is by conduction in the axial direction. The energy equation for packed bed system can be described as:

- **For HTF:**

$$\varepsilon(\rho c)_f \left(\frac{\partial T_f}{\partial t} + u \frac{\partial T_f}{\partial x} \right) = \frac{\partial}{\partial x} \left(k_{fx}^* \frac{\partial T_f}{\partial x} \right) + U.A\left(T_s - T_f\right) \tag{8}$$

- **For solid material**

$$(1-\varepsilon).(\rho c)_s \frac{\partial T_s}{\partial t} = \frac{\partial}{\partial x} \left(k_{sx}^* \frac{\partial T_s}{\partial x} \right) + U.A\left(T_{HTF} - T_s\right) \tag{9}$$

The HTF effective thermal conductivity in the axial direction k_{fx}^* is calculated from the following expressions [**34]**:

$$\begin{cases} k_{fx}^* = 0.7\,\varepsilon\, k_f & for \quad \mathrm{Re}_p \le 0.8 \\ k_{fx} = 0.5\,\mathrm{Pr}_f\,\mathrm{Re}_p\, k_f & for \quad \mathrm{Re}_p \succ 0.8 \end{cases} \tag{10}$$

The solid effective thermal conductivity in the axial direction is calculated from [**50]**:

$$k_{sx}^* = k_{efx} - k_{fx} \tag{11}$$

The axial effective thermal conductivity can be calculated from [**50**]:

$$\frac{k_{efx}}{k_f} = \frac{k_e^0}{k_f} + 0.5\,\mathrm{Pr}_f\,\mathrm{Re}_p \qquad \textbf{(12-a)}$$

where k_e^0 is the stagnation effective thermal conductivity calculated from:

$$\frac{k_e^0}{k_f} = \left(\frac{k_s}{k_f}\right)^m \text{ where } m = 0.280 - 0.757\log\varepsilon - 0.057\log\left(\frac{k_s}{k_f}\right) \qquad \textbf{(12-b)}$$

For packed bed, Nusselt number is frequently used to calculate the inter-phase heat transfer coefficient between the HTF and the solid particles. A number of correlations for the Nusselt number are available in the literature **[11].** Beek **[51]** propose the following correlation (**Eq.13**) which is valid over the porosity range $0.35 \le \varepsilon \le 1$ and up to a Reynolds number of 10^5:

$$\begin{aligned} Nu = {} & \left(7 - 10.\varepsilon + 5.\varepsilon^2\right).\left(1 + 0.7\,\mathrm{Re}_f^{0.2}\,\mathrm{Pr}_f^{0.33}\right) \\ & + \left(1.33 - 2.44\varepsilon + 1.2\varepsilon^2\right).\mathrm{Re}_f^{0.7}.\mathrm{Pr}_f^{0.33} \end{aligned} \qquad \textbf{(13)}$$

2.4 Model with thermal gradient inside the solid particles (Model 4)

The concentric dispersion model takes into account the thermal gradients inside the solid particles and neglects the thermal transfers between the solid particles and, therefore, the variation of the solid particles temperature will be due only to the heat transfer between the HTF and the packed bed. As a result, the energy equation of the packed bed can be described as follows:

- **For HTF**

$$\varepsilon(\rho c)_f\left(\frac{\partial T_f}{\partial t} + u\frac{\partial T_f}{\partial x}\right) = \frac{\partial}{\partial x}\left(k_{fx}^* \frac{\partial T_f}{\partial x}\right) + UA\left(T_s(r=R) - T_f\right) \qquad \textbf{(14)}$$

- **For solid particle**

$$(\rho c)_s \frac{\partial T_s}{\partial t} = k_s \left[\frac{\partial^2 T_s}{\partial r^2} + \frac{2}{r} \frac{\partial T_s}{\partial r} \right] \quad \textbf{(15)}$$

2.5 The total amount of heat stored in the packed bed

The total amount of heat stored in the cylindrical packed bed represents the heat stored in the HTF (air) plus the heat stored in the solid particles, but since $\rho_s c_c$ □ $\rho_f c_f$, Q(t) can be approximated as the heat stored in the solid material storage only:

$$Q(t) = \frac{\pi . d^2}{4} (1 - \varepsilon) \rho_s c_c \int_0^H (T_s - T_{ini}) dx \quad \textbf{(16)}$$

3- Boundary and initial conditions

3.1 Initial condition

The initial condition for all the models is that the initial packed bed temperature has to be uniform, indicating by T_{ini} :

$$T_f(x,0) = T_s(x,0) = T_{ini} \quad \textbf{(17)}$$

3.2 Boundary conditions

The boundary conditions of all models should be physically identical in such a way to be able to perform a comparison and to discuss any differences between the various models.
At the entrance of the packed bed and at time t = 0, the HTF has the following temperature:

$$T_f(0,t) = T_{inlet} \quad \textbf{(18)}$$

Adiabatic conditions for the HTF at the exit of the packed bed and they are expressed by Eq.18:

$$\frac{\partial T_f\left(x=H,t\right)}{\partial x}=0 \quad \textbf{(19)}$$

The adiabatic conditions for the solid particles at the inlet and the outlet of the packed bed are expressed by Eq.19:

$$\frac{\partial T_s\left(0,t\right)}{\partial x}=\frac{\partial T_s\left(H,t\right)}{\partial x}=0 \quad \textbf{(20)}$$

If we consider a thermal gradient inside the solid particles, we have to introduce two other boundary conditions:

$$\frac{\partial T_s}{\partial r}=0 \quad for \quad r=0 \quad \textbf{(21)}$$

and

$$\lambda_s \frac{\partial T_s}{\partial r}=U\left(T_f-T_s\left(r=R\right)\right) \quad for \quad r=R \quad \textbf{(22)}$$

4- Numerical procedure

Based on the developed physical models, a numerical tool in the FORTRAN 90 environment has been developed. It enables the prediction of thermal performance of the packed bed during the charging and discharging process.

The energy equations that describe the four physical models with the corresponding initial and boundary conditions has been numerically solved by using the control volume finite difference technique **[52-53].** The packed bed is partitioned into several adjacent control volumes, where the grid points are located at the center of each control volume. The time derivations are determined by using totally implicit time integration. The Upwind scheme is adopted for discretization of the convection terms and the central difference scheme is used for discretization of the diffusion term. The obtained discrete equations were iteratively solved at each time step using the tridiagonal matrix algorithm (TDMA). At each time step, convergence was supposed to be achieved once the temperature residuals become lower than

some predefined values tol_f and tol_{pcm} i.e. $\left|\frac{T_{f,P}^{k+1}-T_{f,P}^{k}}{T_{f,P}^{k}}\right| \prec tol_f$ and $\left|\frac{T_{s,P}^{k+1}-T_{s,P}^{k}}{T_{s,P}^{k}}\right| \prec tol_s$. In this work, all calculations were performed with $tol_f = tol_s = 10^{-5}$.

5- Numerical simulations and experimental validation

The physical models are verified using the experimental data provided by Meier et al. **[54].** The experiment involves a 3-hour charging process carried out in a laboratory storage facility. The dimensions of this experimental device and its functional characteristics are described in **Table 1**. Due to the small ratio of the tank diameter to solid particles diameter ratio (D/d = 7.4), the influence of the near wall **effects** on the measured data is important. In fact, some of the air flow is directed through this slightly non-porous region and therefore doesn't participate in heat transfer by convection inside the packed bed. In order to consider these effects, Meier et al. **[54]** proposed to adjust the mass velocity G used in the calculations (See **Table 1**). As illustrated in **Figures 2-a, 2-b, 2-c** and **2-d**, the computed temperature profiles inside the packed bed are approximately in line with the experimental profiles registered when the mass effective flow was decreased by 10%. It can also be noted that the two models (Model 3 and Model 4) that take into account heat conduction inside the solid particles are in good agreement with the experiment. On **Fig. 3**, we have reported the variation of the HTF temperature at the outlet of the tank for the four models (Model 1, Model 2, Model 3 and Model 4). We can observe that the HTF temperature at the outlet of the tank provided by models 3 and 4 is lower than that calculated with models 1 and 2. These results can be explained by the impact of the heat conduction within the solid particles on the thermal behavior of the packed bed. We can also conclude that the heat conduction inside the HTF can be neglected without introducing any particular error on the thermal behavior of the packed bed.

Figs.4-a, 4-b, 4-c and **4-d** exhibit the numerical results of the temperature evolution of the HTF and the solid particles inside the packed bed. We note that for all models the temperature profiles increase progressively along the height of the packed bed. This behavior is typical of a plug flow system, where

the front travels in the axial direction. The difference between the HTF and solid temperature profiles can be considered negligible.

It is interesting to note that models with negligible thermal gradient inside solid particles can be adopted when the thermal conduction resistance in the solid of the packed bed is negligible compared to the thermal convection resistance. This condition is assessed thanks to the dimensional Biot number:

$$Bi = \frac{U.d}{k_s} \leq 0.1 \quad \textbf{(23)}$$

To verify the validity of Equation 23, we tested Model 4 for two values of thermal conductivity of the solid material (0.2 W/m.K) and (2.5 W/m.K) (**see Figs 5-a and 5-b)** for the same value of U**.** The diameter of the solid particle is assumed to be 0.06 m. The thermophysical properties of HTF and solid particles properties are maintained constant (see **Table.1**). We note that the thermal diffusion in the solid particle cannot be neglected when the thermal conductivity is 0.2 W/(m.K). Consequently, models in which the thermal diffusion inside the solid particles is neglected (i.e. $Bi \leq 0.1$) can be adopted to describe the thermal behavior of the packed bed.

The single phase model is said to work when the thermal conductivity and thermal capacity of the solid material are high compared to the heat transfer fluid. It is evident that these conditions are usually respected in many storage materials like alumina material. The volumetric heat capacity of alumina is 2500 higher than air. The thermal conductivity of alumina is 1300 times higher than the air. Thus, thermal equilibrium is a plausible hypothesis in the air/alumina system, which implies that the porous media can be reasonably considered as homogeneous system.

6- Results and discussion

The most important factors that affect the thermal behavior of the packed bed for sensible heat storage are the thermophysical properties of the solid storage material, the size of the solid material, the mass velocity of the HTF and the porosity of the bed. In the coming paragraphs, we will examine the effect of each of these parameters on the thermal behavior of the packed bed.

6-1 Influence of the thermophysical properties of the solid material

The principal problem in the use of solid materials for thermal energy storage systems is the relatively large size of the storage tank. However, this can be reduced by using storage materials with high thermal capacity and resisting to high temperature levels.

It is important to mention that solid materials with high thermal diffusivity ($\frac{k_s}{\rho_s . c_s}$), but low effusivity ($\sqrt{k_s . \rho_s . c_s}$) seem to be the most adequate for sensible heat storage systems.

Table 2 illustrates that certain metallic materials look as good candidates as mineral materials. However, both availability and cost-effectiveness should also be considered in the evaluation and, in this regard, mineral materials have certain merits.

The density and the specific heat capacity of the solid material are also among the important properties in the design and the choice of the solid storage materials. The impact of the density of the solid storage material on the energy stored inside the packed bed was reported in **Fig.6**. The values of the thermal conductivity and specific heat capacity are maintained at their nominal values (see **Table 1**). The higher rate of thermal charging and higher storage capacity of the denser material is evident (see **Fig.6**). It should also be noted that the stored energy increases in a nearly linear manner over time during the charging period until it reaches a maximum value, and that the linear part of the curve increases with the increase in solid material density.

The influence of the specific heat capacity of the storage material on the thermal behavior of the packed bed was analyzed for values varying from 50 to 1068 J/kg.K (see **Fig.7**). A significant improvement in the energy storage level and capacity with an increase in the heat capacity of the solid storage material is observed.

6-2 Influence of the solid material diameter

Fig.8 displays the influence of the solid material particle diameter on the thermal behavior of the tank. The decrease in the size of the solid particles leads to an increase in their number and therefore to an improvement in the heat exchange surface between the solid particles and the

HTF. We can also notice that for a given particle size rise, there is a correlative rise in the charging time.

6-3 Influence of the HTF mass velocity

The effect of the mass velocity of HTF on the thermal behavior of the packed-bed is presented in **Fig.9**.As shown in **Fig.9**, the higher the HTF mass velocity, the shorter the charge time. The rise in the mass velocity HTF leads to an improvement in the thermal transfer coefficient between HTF and solid storage material. For the three HTF mass velocity under study, all sensible energy is stored.

6-4 Influence of the porosity

For a packed bed having a certain volume and a certain diameter of solid particles, its porosity determines the quantity of thermal energy that can be stored, the superficial area of the heat transfer between the solid particle and HTF per unit volume and the pressure drop along the packed bed axis. Hence for a bed of certain particle diameter, a range of variation of the porosity can obtained by only varying the filling arrangement of the bed. A reduction in porosity causes an increase in the mass of solid particles in the tank, an improvement in the thermal storage capacity of the bed, as well as an increase in the thermal transfer area and the pressure drop over the packed bed. As a result, an increase in the bed porosity leads also to an increase in the duration of the charging process (see **Fig.10**).

7. Thermal optimization of the packed bed

The principal objective of a thermal energy storage system is to ensure a good heat transfer efficiency during charging and discharging process with acceptable pumping imperatives.

By adopting the concepts of heat exchangers [**56-57**] and using the height *H* of the packed bed as a characteristic length, the number of transfer units (NTU) of the bed can be estimated as:

$$NTU = 6.(1-\varepsilon).St.\frac{H}{d} \quad \textbf{(24)}$$

where St is the Staton number ($St = \frac{U}{G.c_f}$) related to the solid particle Nusselt number Nu_s and solid particle Peclet number Pe_s as follows:

$$St = \frac{Nu_s}{Pe_s} \quad \textbf{(25)}$$

NTU number is a dimensionless parameter whose amplitude affects the thermal performance of the packed bed. High values of NTU improve the packed bed effectiveness and ameliorate the charging and discharging rates.

The Ergun equation **[58-59]** is one of the most correlation used to estimate the pressure drop through packed beds of spherical solids particles.

$$\frac{\Delta P}{H} = A.\frac{(1-\varepsilon)^2}{\varepsilon^3}\frac{\mu_f.\mathrm{u}_e}{d^2} + B.\frac{(1-\varepsilon)}{\varepsilon^3}.\frac{\rho_f.\mathrm{u}_e^2}{d} \quad \textbf{(26)}$$

where μ_f is the dynamic viscosity of the HTF, u_e is the superficial bed velocity (i.e. the average velocity of the HTF in an empty bed), ρ_f is the density of the HTF, A is 150 and B is 1.75. The first term on the right-hand side refers to the viscous energy losses that govern during laminar flow and the second term accounts for kinetic losses that dominate in the turbulent regime.

Figs. (11-a) and (11-b) illustrate the change in the NTU and the pressure drop across the packed bed with $\frac{H}{d}$ for various values of the mass velocity G of the HTF. It can be seen that the value of NTU rises with the rise in the mass velocity G of the HTF. For the identical value of G, the value of NTU becomes higher as the diameter of the particles is reduced. It is important to note that the rise of NTU with the increase in $\frac{H}{d}$ is significant for lower values of G. Regarding the pressure drop, important values of pressure drop are observed for higher values of G. The rate of increase of pressure drop with the rise of $\frac{H}{d}$ is expected to be negligible at relatively small values of G. From this assessment, it can be seen that, generally,

the selection of relatively small diameter solid particles is advantageous in terms of heat transfer rates and pumping requirements at low values of the mass velocity of the HTF.

This analysis shows that, in general, for a relatively small values of the mass velocity of the HTF, the utilization of solid particles with small diameter is beneficial in terms of thermal packed bed efficiency and pumping performances.

8. Conclusion

Numerical simulations were carried out with four physical models to describe the thermal behavior of the packed bed for sensible heat storage. It is found that the physical with thermal gradient inside the solid particles have to be considered and adopted only when there is a need for detailed information inside the solid particle (like thermal diffusion). The influence of various parameters on the thermal behavior and the pressure drop over the packed bed during the charging process is reported and discussed. It is found that :

- The thermal behavior of the packed is strongly influenced by the mass velocity of the HTF, the solid particle diameter, and the porosity of the bed ;
- At relatively small values of the mass velocity of the HTF, the choice of solid particles with small diameter is profitable in terms of thermal packed bed efficiency and pumping requirements.

Nomenclature

A	capsule area, m^2
Bi	Biot number
c	specific heat, $J.kg^{-1}.K^{-1}$
d	capsule diameter, m
D	bed diameter, m
G	mas velocity, $kg.m^2.s^{-1}$
H	bed height, m
k	thermal conductivity, $W.m^{-1}.K^{-1}$
Nu	Nusselt number
P	pressure, Pa
Pe	Peclet number
Pr	Prandtl number
Q	heat storage
Re	Reynolds number
R	radius, m
r	radial coordinate, m
St	Staton number
T	temperature, K
t	temps, s
U	heat transfer coefficient, $W.m^{-2}.K^{-1}$
u	velocity, $m.s^{-1}$
x	spatial coordinate, m

Greek symbols

ε	bed porosity
μ	dynamic viscosity, Pa.s
ρ	density, kgm^{-3}

Subscripts

e	effective
f	fluid
HTF	hot thermal fluid

ini	initial
m	mixture
p	particle
pcm	phase change material
s	solid

References

[1] S. Kuravi, J. Trahan, D. Y. Goswami, M. M. Rahman, E. K. Stefanakos, Thermal energy storage technologies and systems for concentrating solar power plants, Progress in Energy and Combustion Science 39 (2013) 285-319

[2] T. Kousksou, P. Bruel, A. Jamil, T. El Rhafiki, Y. Zeraouli, Energy storage: Applications and challenges, Solar Energy Materials and Solar Cells, 120 (2014) 59-80

[3] A. Arteconi, N.J. Hewitt, F. Polonara, State of the art of thermal storage for demand-side management, Appl. Energy 93 (2012) 371-389.

[4] T. Kousksou, P. Bruel, G. Cherreau, V. Leoussoff, T. El Rhafiki, PCM storage for solar DHW: From an unfulfilled promise to a real benefit, Solar Energy 85 (2011) 2033-2040.

[5] X. Chen, Z. Zhang, C. Qi, X. Ling, H. Peng, State of the art on the high-temperature thermochemical energy storage systems, Energy Conversion and Management, 177 (2018) 792-815.

[6] C. Zauner, F. Hengstberger, Benjamin Mörzinger, R. Hofmann, H. Walter, Experimental characterization and simulation of a hybrid sensible-latent heat storage, Applied Energy 189 (2017) 506–519

[7] K. Bataineh, A. Gharaibeh**,** Optimal design for sensible thermal energy storage tank using natural solid materials for a parabolic trough power plant, Solar Energy 171 (2018) 519-525.

[8] U. Pelay, L. Luo, Y. Fan, D. Stitou, M. Rood, Thermal energy storage systems for concentrated solar power plants, Renewable and Sustainable Energy Reviews 79 (2017) 82-100.

[9] R. Tiskatine, R. Oaddi, R. Ait El Cadi, A. Bazgaou, L. Bouirden, A. Aharoune, A. Ihlal, Suitability and characteristics of rocks for sensible heat storage in CSP plants, Solar Energy Materials and Solar Cells 169 (2017) 245-257.

[10] A. Kumar, M-H. Kim, Solar air-heating system with packed-bed energy-storage systems, Renewable and Sustainable Energy Reviews 72 (2017) 215-227.

[11] A. de Gracia, L. F. Cabeza**,** Numerical simulation of a PCM packed bed system: A review, Renewable and Sustainable Energy Reviews 69 (2017) 1055–1063.

[12] T. Esence, A. Bruch, S. Molina, B. Stutz, J-F Fourmigué, A review on experience feedback and numerical modeling of packed-bed thermal energy storage systems, Solar Energy 153 (2017) 628–654.

[13] A. Gil, M. Medrano, I. Martorell, A. Lazaro, P. Dolado, B. Zalba, L. Cabeza, State of the art on high temperature thermal energy storage for power generation. Part1 d concepts, materials, and modellization, Renew. Sustain. Energy Rev. 14 (2010) 31-55.

[14] KAR Ismail, R. Stuginsky, A parametric study on possible fixed bed models for PCM and sensible heat storage, Appl. Therm. Eng. 19 (1999) 757–88.

[15] T.E.W. Schumann, Heat transfer: a liquid flowing through a porous prism, J. Franklin Inst. 208 (1929) 405–416.

[16] H. Martin, Low peclet number particles- to-fluid heat and mass transfer in packed beds, Chem. Engng. Sci. 33(1978) 913–921.

[17] D.J. Gross, C.E. Hickox, C.E. Hackett, Numerical simulation of dual-media thermal energy storage systems, Trans. ASME, J. Solar Energy Engng. 102 (1980) 287–297.

[18] D.E. Beasley, J.A. Clark, Transient response of a packed bed for thermal energy storage, International Journal of Heat and Mass Transfer 27 (1984) 1659–1699.

[19]D. Handley, P.J. Heggs, The effect of thermal conductivity of the packing material on transient heat transfer ina fixed bed, Int. J. Heat Mass Transfer 12 (1969) 549–570.

[20]C.G. Furnas, Heat transfer from a gas stream to a bed of broken solids II, Ind. Engng. Chem. 22 (1930) 721–731.

[21] D.J. Gunn, Transfer of heat or mass to particles in fixed and fluidised beds. Int. J. Heat Mass Transf. 21 (1978) 467–476.

[22] D. Vortmeyer, R.J. Schaefer, Equivalence of one and two–phase models for heat transfer processes in packed beds: one dimensional theory, Chem. Engng. Sci. 29 (1974) 485–491.

[23] D. Vortmeyer, W. Adam, Steady-state measurements and analytical correlation of axial effective thermal conductivities in packed beds at low gas flow rates, Int. J. Heat Mass Transfer 27 (1984) 1465–1472.

[24]R.W. Persons, J.A. Due, J.W. Mitchell, Comparison of measured and predicted rock bed storage performance, Solar Energy 24 (1980) 199–201.

[25]M.M. Melanson, A.G. Dixon, Solid conduction in low dt/dp beds of spheres, pellets and rings, Int. J. Heat Mass Transfer 28 (1985) 383–394.

[26] K.G.T. Hollands, SullivanHF, E.C. Shewen, Flow uniformity in rock bed, Solar Energy 32 (1984) 343–348.

[27]J.P. Coutier, E.A. Faber, Two application of a numerical approach of heat transfer processes within rock beds, Solar Energy 29 (1982) 451–462.

[28]M. Raiz, Transient analysis of packed-bed thermal storage systems, Solar Energy 21 (1978) 123–128.

[29]E.F. Sowell, R.L. Curry, A convolution model of the rock bed thermal storage units, Solar Energy 24 (1980) 441–449.

[30]H. Littman, R.G. Barile, A.H. Pulsiver, Gas-particles heat transfer in packed beds at low reynolds numbers, Ind. Engng. Chem. Fundam. 7 (1968) 554–561.

[31] S.N. Gupta, R.B. Chaube, S.N. Upadhyay, Fluid-particle heat transfer in fixed and fluidized beds, Chem. Engng. Sci. 29 (1974) 839–843.

[32] O. Maaliou, B.J. McCoy, Optimization of thermal energy storage in packed columns, Solar Energy 34 (1985) 35–41.

[33] G. Alva, Y. Lin, G. Fang, An overview of thermal energy storage systems, Energy 144 (2018) 341-378

[34] Gang Li, Sensible heat thermal storage energy and exergy performance evaluations, Renewable and Sustainable Energy Reviews 53 (2016) 897–923.

[35] M. Hanchen, S. Brückner, A. Steinfeld, High-temperature thermal storage using a packed bed of rocks - heat transfer analysis and experimental validation, Appl. Therm. Eng. 31 (2011) 1798-1806.

[36] S.L. Aly, A.I. El-Sharkawy, Effect of storage medium on thermal properties of packed bed. Heat Recovery Syst. CHP 10 (1990) 509–17.

[37] M. Rady, Granular phase change materials for thermal energy storage: experiments and numerical simulations. Applied Thermal Engineering 29 (2009) 3149-4159.

[38] M. Wu, M. Li, C. Xu, Y. He, W. Tao, The impact of concrete structure on the thermal performance of the dual-media thermocline thermal storage tank using concrete as the solid medium. Applied Energy 113 (2014)1363–71.

[39] B. Xu, P.W. Li, C.L. Chan, Extending the validity of lumped capacitance method for large Biot number in thermal storage application. Solar Energy 86 (2012) 1709–24.

[40] Z. Liao, G. Zhao, G. Xu, G. Yang, Y. Jin, X. Ju, X. Du, Efficiency analyses of high temperature thermal energy storage systems of rocks only and rock-PCM capsule combination. Solar Energy 162 (2018) 153-164.

[41] D. Brosseau, J.W. Kelton, D. Ray, M. Edgar, K. Chisman, B. Emms, Testing of thermocline filler materials and molten salt heat transfer fluids for thermal energy storage systems in parabolic trough power plants. J. Sol. Energy Eng. Trans. ASME 127 (2005) 109-116.

[42] M. Cascetta, G. Cau, P. Puddu, F. Serra, Numerical investigation of a packed bed thermal energy storage system with different heat transfer fluids, Energy Procedia 45 (2014) 598-607.

[43] M.A. Izquierdo-Barrientos, C. Sobrino, J.A. Almendros-Ibáñez, Modeling and experiments of energy storage in packed bed with PCM. International Journal of Multiphase Flow 86 (2016) 1-9.

[44] F. Ma, P. Zhang, Investigation on the performance of a high-temperature packed bed latent heat thermal energy storage system using Al-Si alloy. Energy Conversion and Management 150 (2017) 500–514.

[45] H. Agalit, N. Zari, M. Maalmi, M. Maaroufi, Numerical investigations of high temperature packed bed TES systems used in hybrid solar tower power plants. Solar Energy 122 (2015) 603–616

[46] C. Xu, Z. Wang, Y. He, F. Bai, Sensitivity analysis of the numerical study on the thermal performance of a packed bed molten salt thermocline thermal storage system. Applied Energy 92 (2012) 65-75.

[47] N. Mertens, F. Alobaid, L. Frigge, B. Epple, Dynamic simulation of integrated rock-bed thermocline storage for concentrated solar power. Solar Energy 110 (2014) 830–842.

[48] P. Klein, T.H. Roos, T.J. Sheer, Parametric analysis of a high temperature packed bed thermal storage design for a solar gas turbine. Solar Energy 118 (2015) 59–73.

[49] K. Niedermeier, L. Marocco, J. Flesch, G. Mohan, J. Coventry, T. Wetzel. Performance of molten sodium vs. molten salts in a packed bed thermal energy storage. Applied Thermal Engineering 141 (2018) 368–377.

[50] N. Wakao, S. Kaguei, Heat and mass transfer in packed beds. Gordon and Braech, New York, 1982.

[51] J. Beek, Design of packed catalytic reactors. Adv. Chem. Eng. 3(1962)203–71.

[52] T. Kousksou, P. Bruel, Encapsulated phase change material under cyclic pulsed heat load, International Journal of Refrigeration 33 (2010) 1648-1656.

[53] T. Kousksou, F. Strub, J. Castaing Lasvignottes, A. Jamil, J.P. Bédécarrats, Second law analysis of latent thermal storage for solar system. Solar Energy Materials and Solar Cells 91 (2007) 1275-1281.

[54] A. Meier, C. Winkler, D. Wuillemin, Experiment for modeling high temperature rock bed storage. Sol. Energy Mater. 24 (1991) 255–264.

[56] N.A.M. Amin, M. Belusko, F. Bruno, An effectiveness-NTU model of a packed bed PCM thermal storage system, Applied Energy 134 (2014) 356-362.

[57] A. Amiri, K. Vafai, Transient analysis of incompressible flow through a packed bed. Int. J. Heat Mass Trans 41 (1998) 4257–79.

[58] F. Kuwahara, A. Nakayama, H. Koyama, A numerical study of thermal dispersion in porous media. J. Heat Trans. 118 (1996) 756–61.

[59] J. Theuerkauf, P. Witt, D. Schwesig, Analysis of particle porosity distribution in fixed beds using the discrete element method. Powder Technol. 165 (2006) 92–9.

Table 1: Dimensions and operational parameters of the experimental setup [54]

Parameter	Value
T_{inlet}	550°C
T_{ini}	20°C
G	0.225 kg/m^2.s
H	1.2 m
D	0.148 m
ε	0.4
d	0.02m
U	0.687 W/ (m^2.K)
ρ_s	2680 kg/m^3
c_s	1068 J/(kg.K)
K_s	2.5 W/(m.K)

Table 2: Thermal diffusivity and effusivity of certain solid storage materials **[9]**

Material	Diffusivity ($m^2.s$)	Effusivity ($Wm^{-2}K^{-1}s^{-1/2}$)
Limestone	$4.8\ 10^{-7}$	993
Standstone	$5.7\ 10^{-7}$	1700
Granite	$8 – 18\ 10^{-7}$	1900 - 2950
Al	$13\ 10^{-6}$	12800
Cast iron	$13\ 10^{-6}$	17173
Cu	$11\ 10^{-5}$	36383

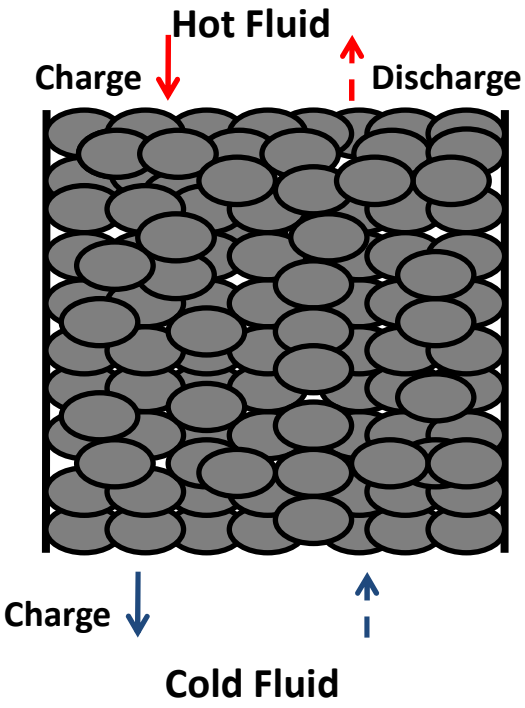

Fig.1 : Sketch of a packed bed thermal storage system

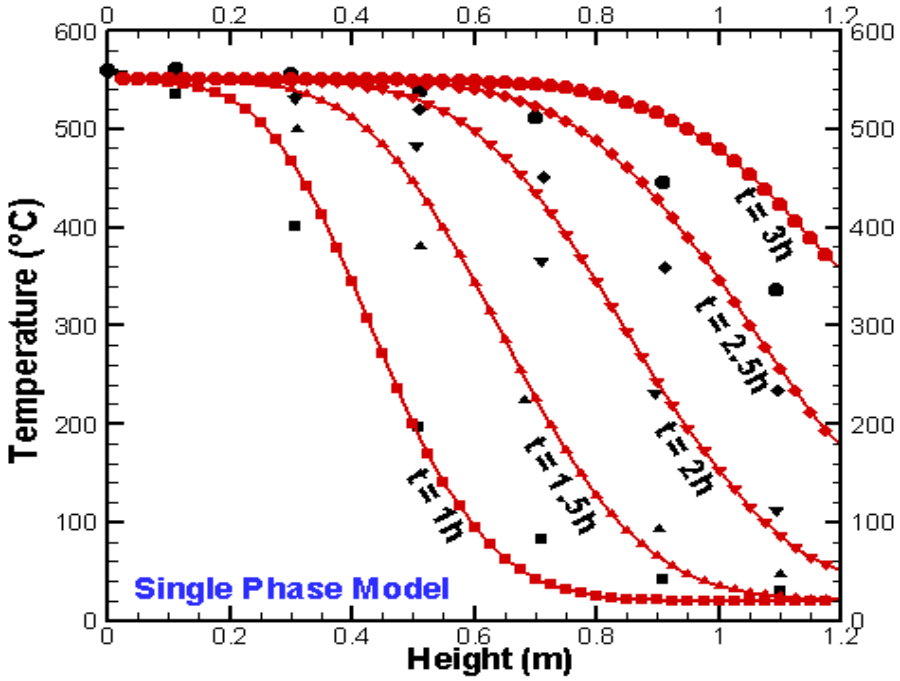

Fig. 2-a: Temperature profile of the HTF during charging process, measurement data (black dots) and calculations (continued line).

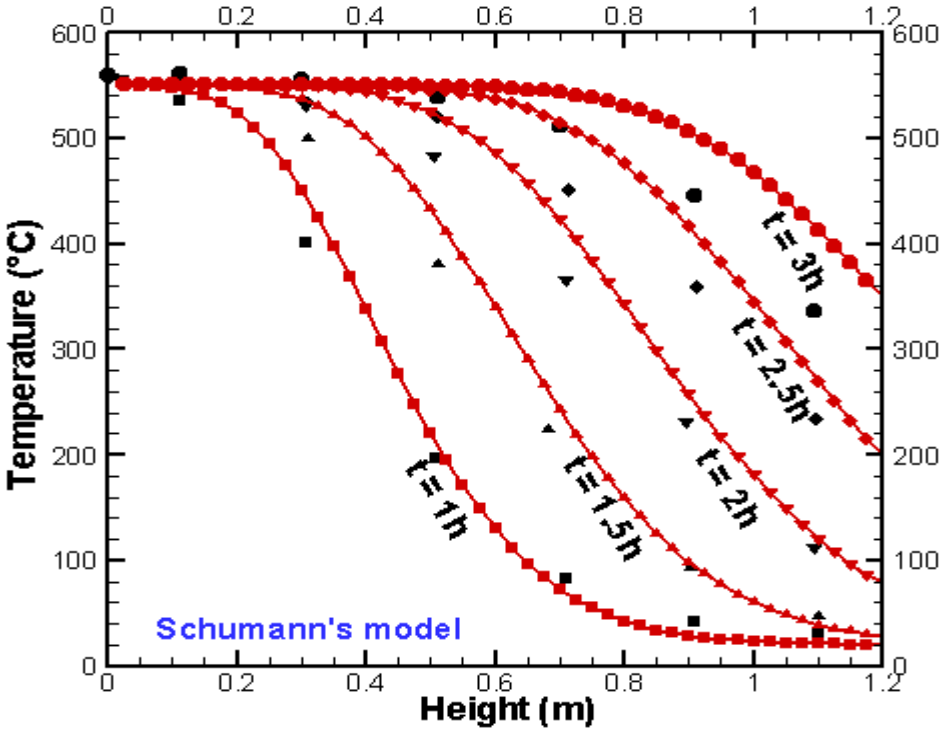

Fig. 2-b: Temperature profile of the HTF during charging process, measurement data (black dots) and calculations (continued line).

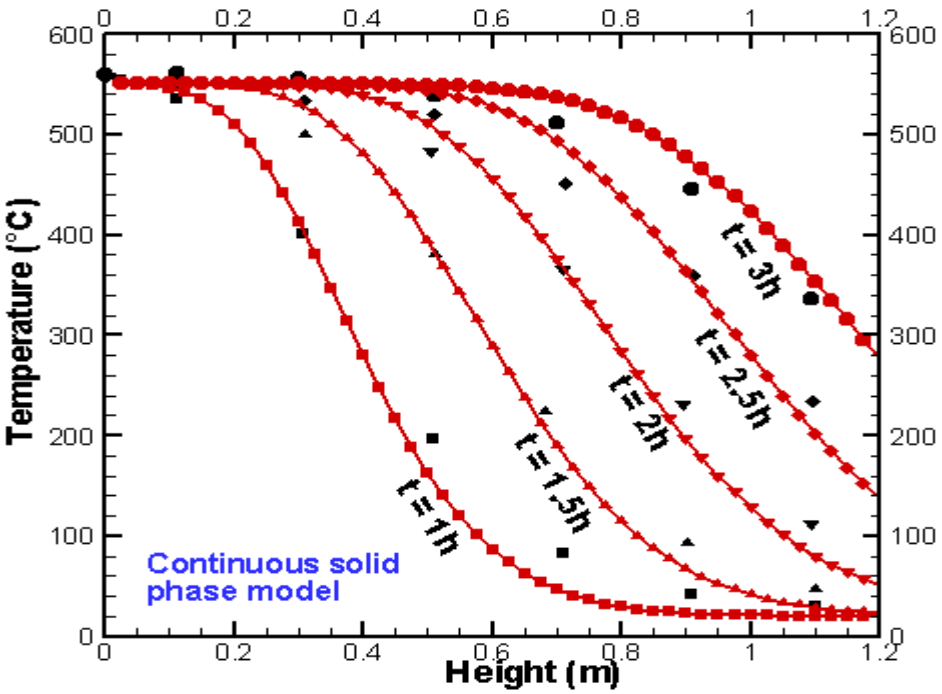

Fig. 2-c: Temperature profile of the HTF during charging process, measurement data (black dots) and calculations (continued line).

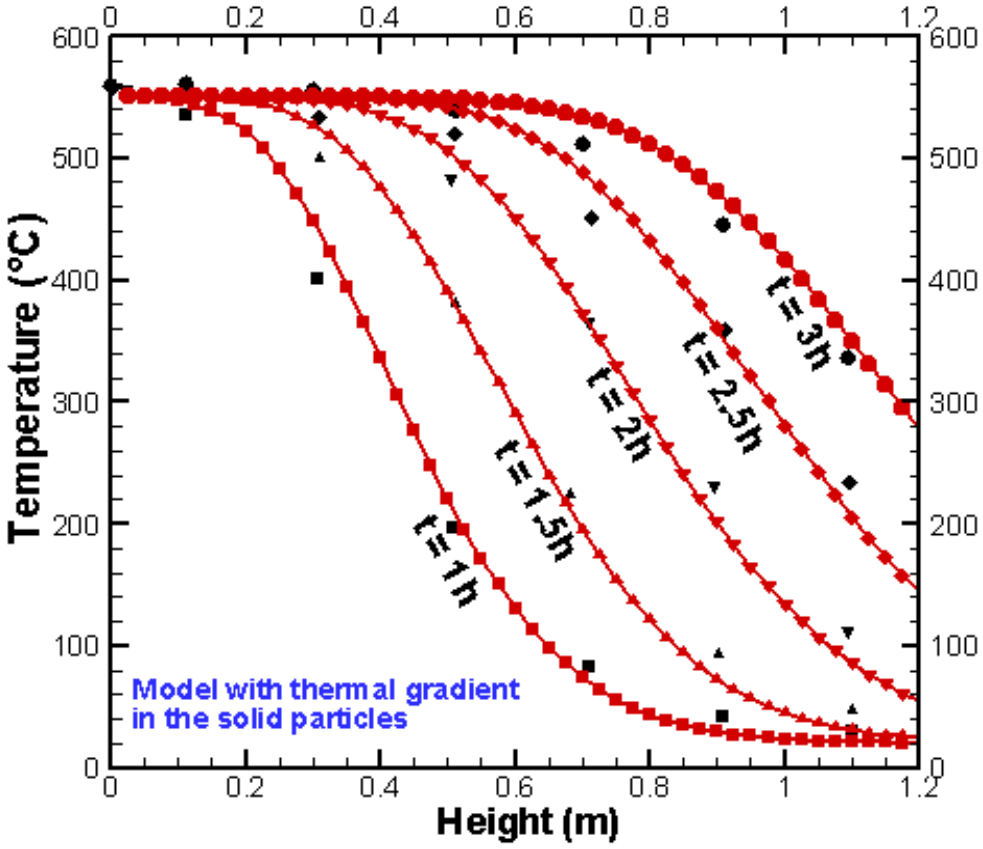

Fig. 2-d: Temperature profile of the HTF during charging process, measurement data (black dots) and calculations (continued line).

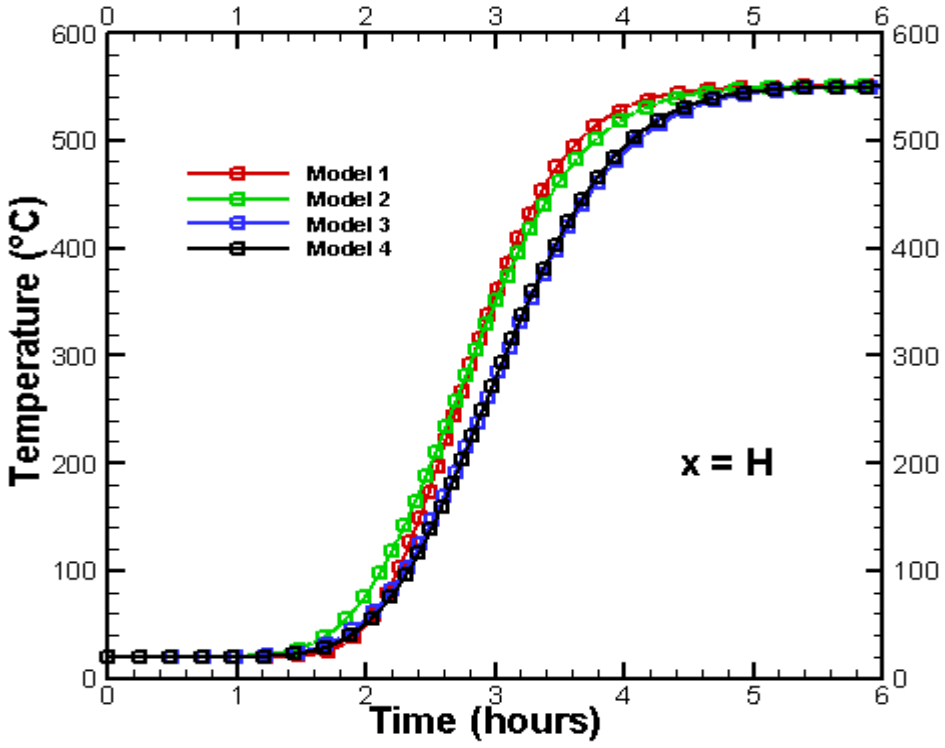

Fig. 3: Temperature profile of the HTF during charging process at the outlet of the packed bed

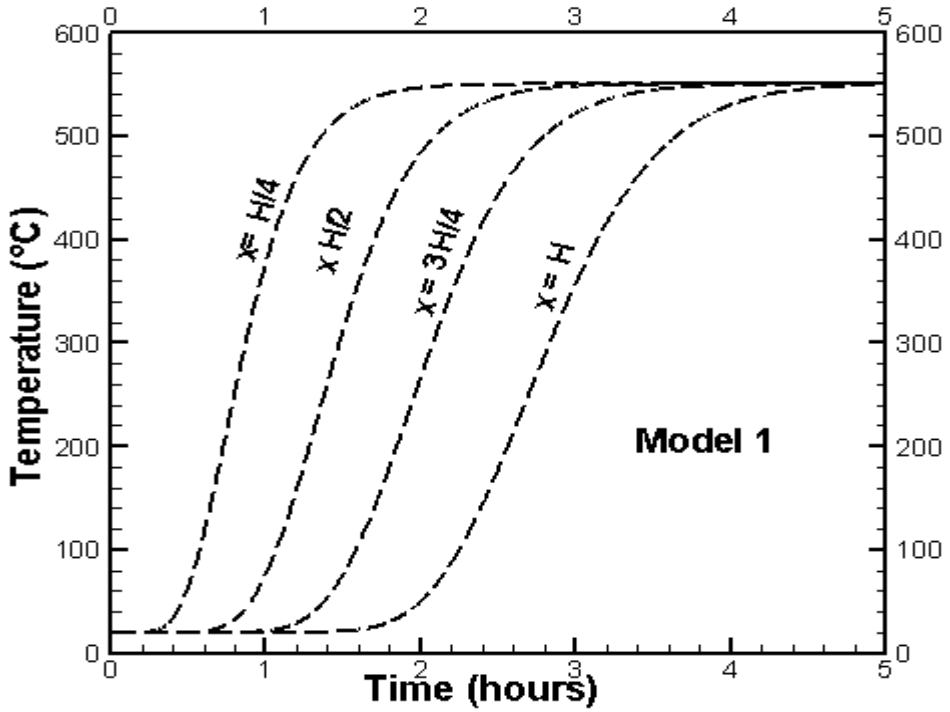

Fig. 4-a: Temperature profile of the HTF during charging process at different positions inside the packed bed

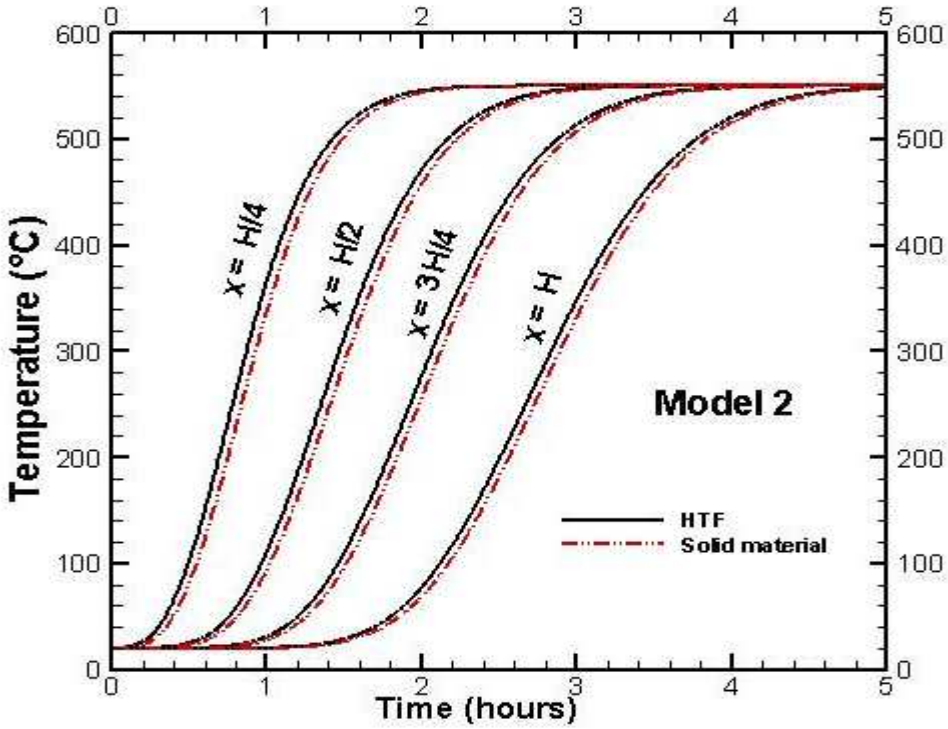

Fig. 4-b: Temperature profile of the HTF during charging process at different positions inside the packed bed

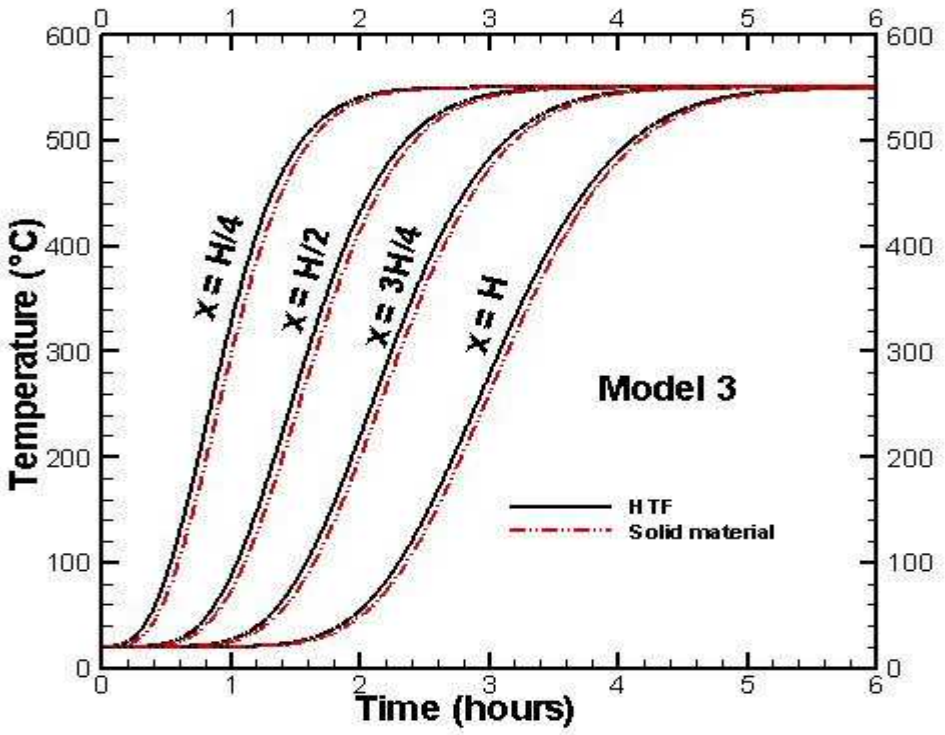

Fig. 4-c: Temperature profile of the HTF during charging process at different positions inside the packed bed

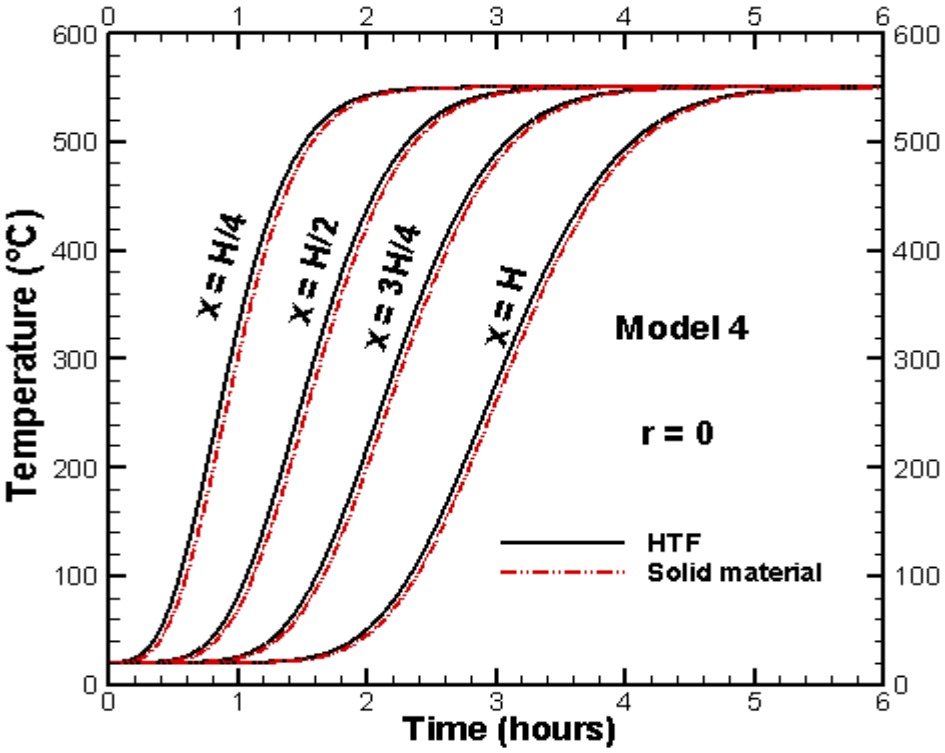

Fig. 4-d: Temperature profile of the HTF during charging process at different positions inside the packed bed

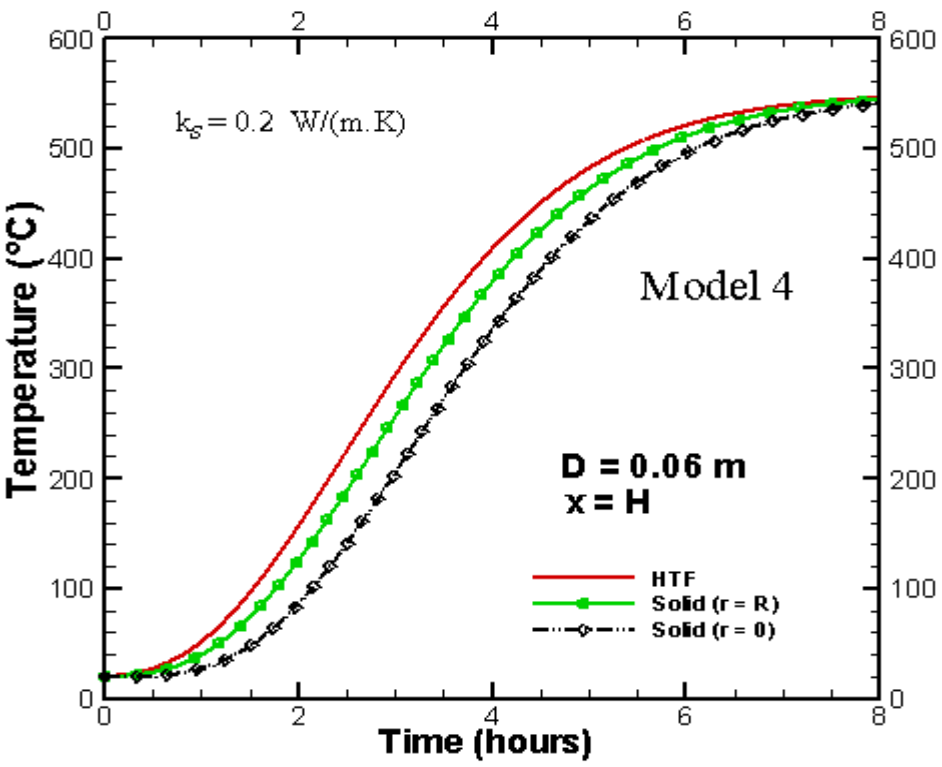

Fig. 5-a: Temperature profile of the HTF during charging process at the outlet of the packed bed

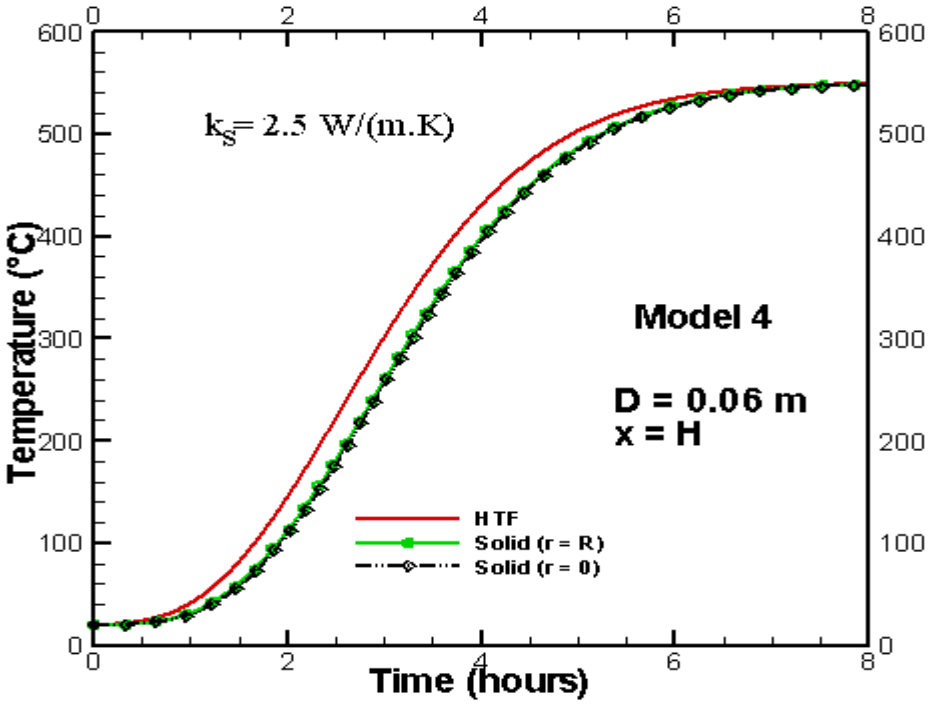

Fig. 5-b: Temperature profile of the HTF during charging process at the outlet of the packed bed

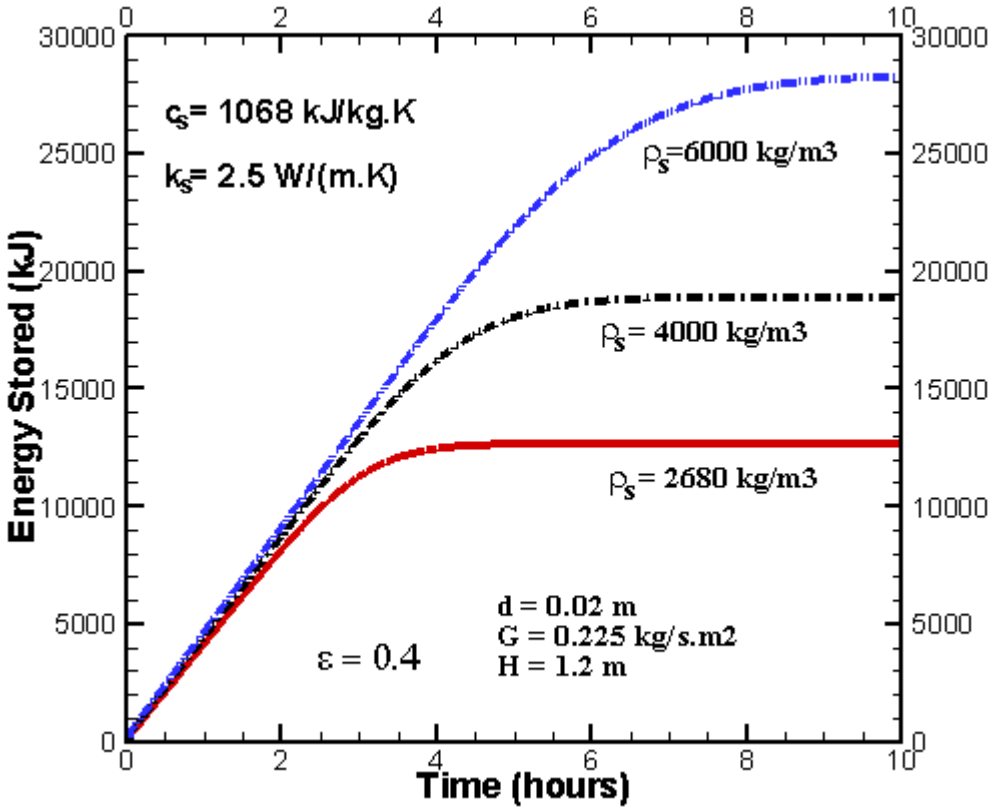

Fig. 6: Variation of energy stored with time for different solid densities

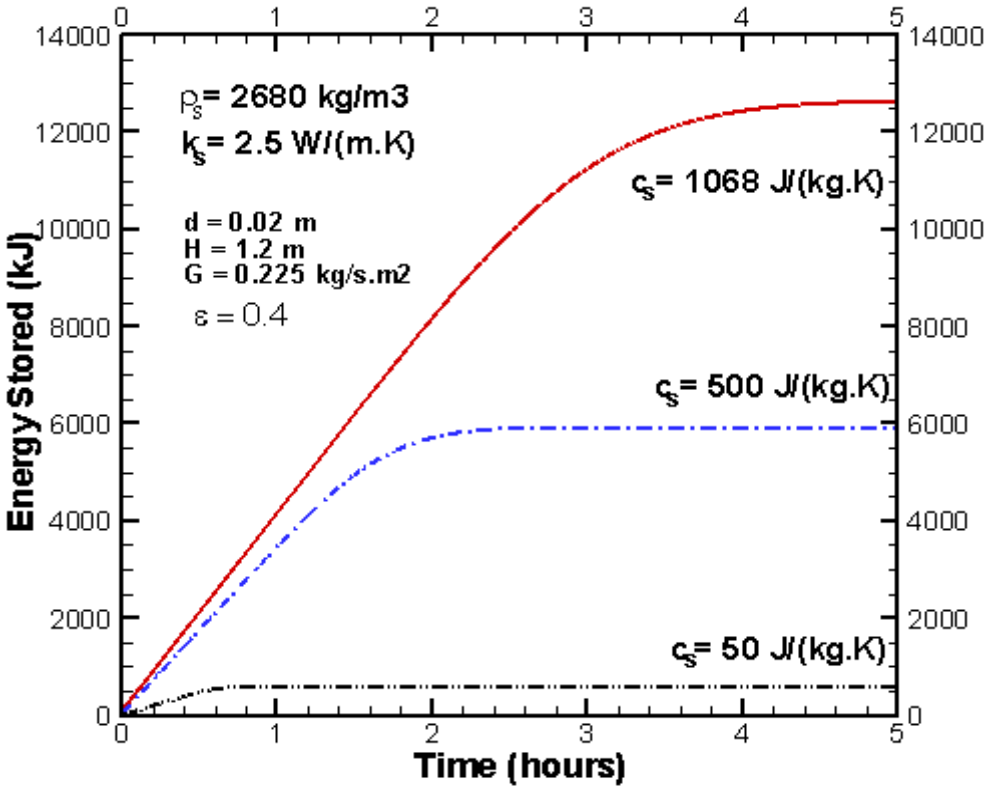

Fig. 7: Variation of energy stored with time for different solid heat capacities

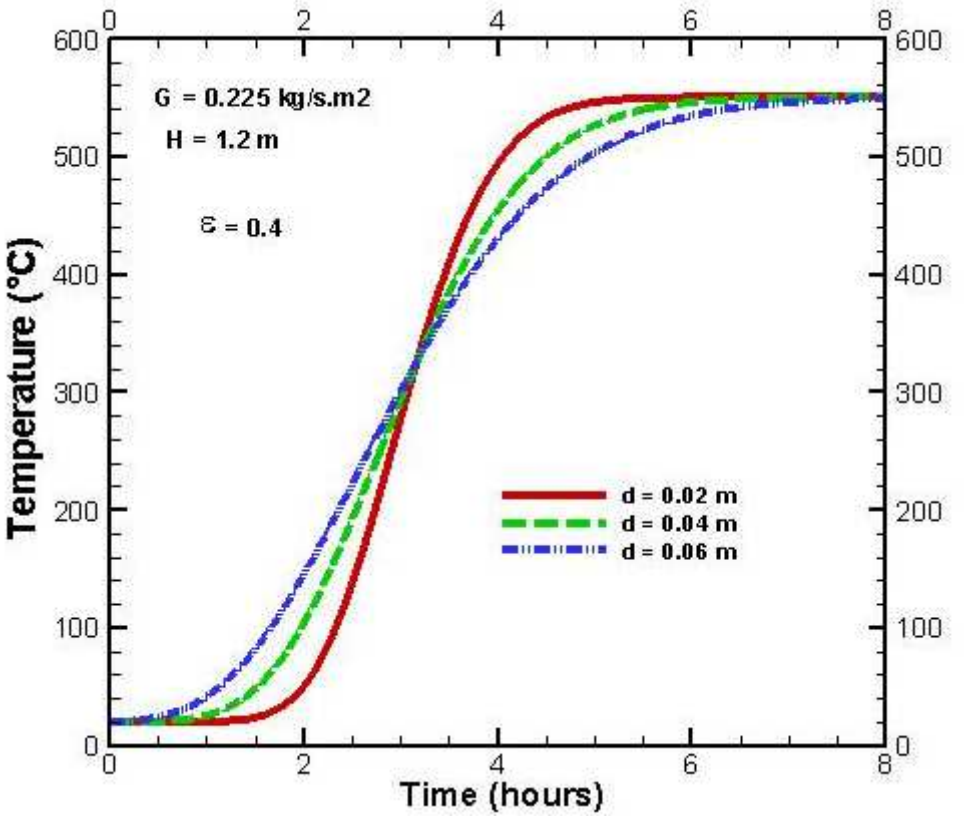

Fig. 8: Effect of the particle diameter on the duration of charging process

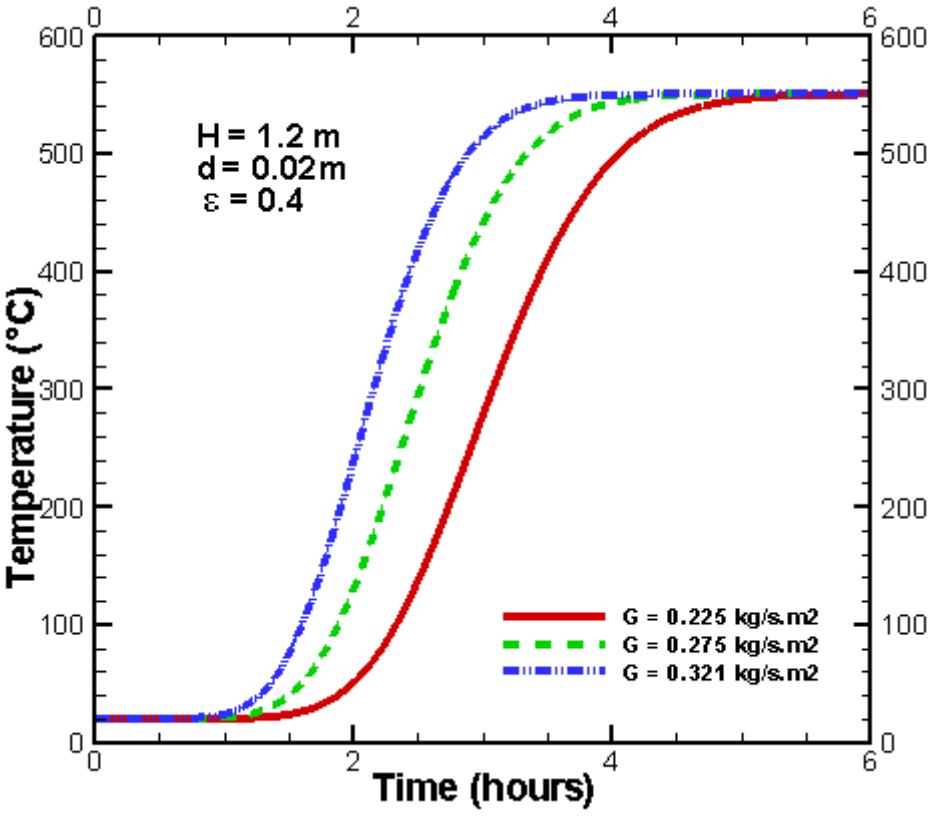

Fig. 9: Effect of the mass flow rate on the duration of charging process

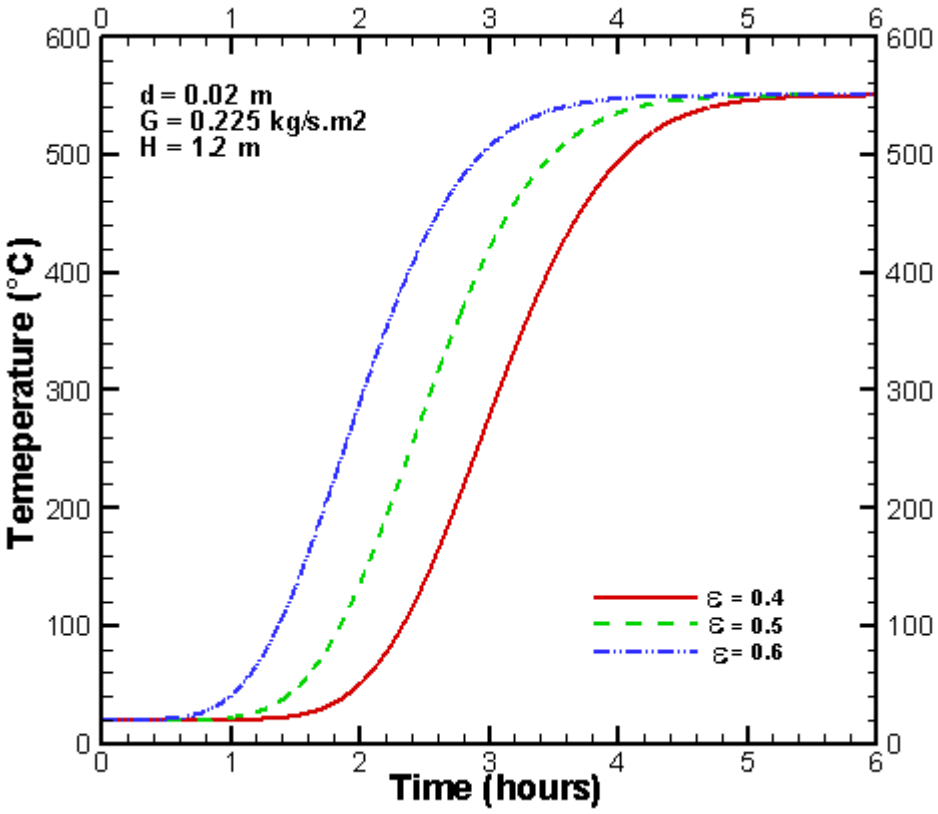

Fig. 10: Effect of the porosity on the duration of the charging process

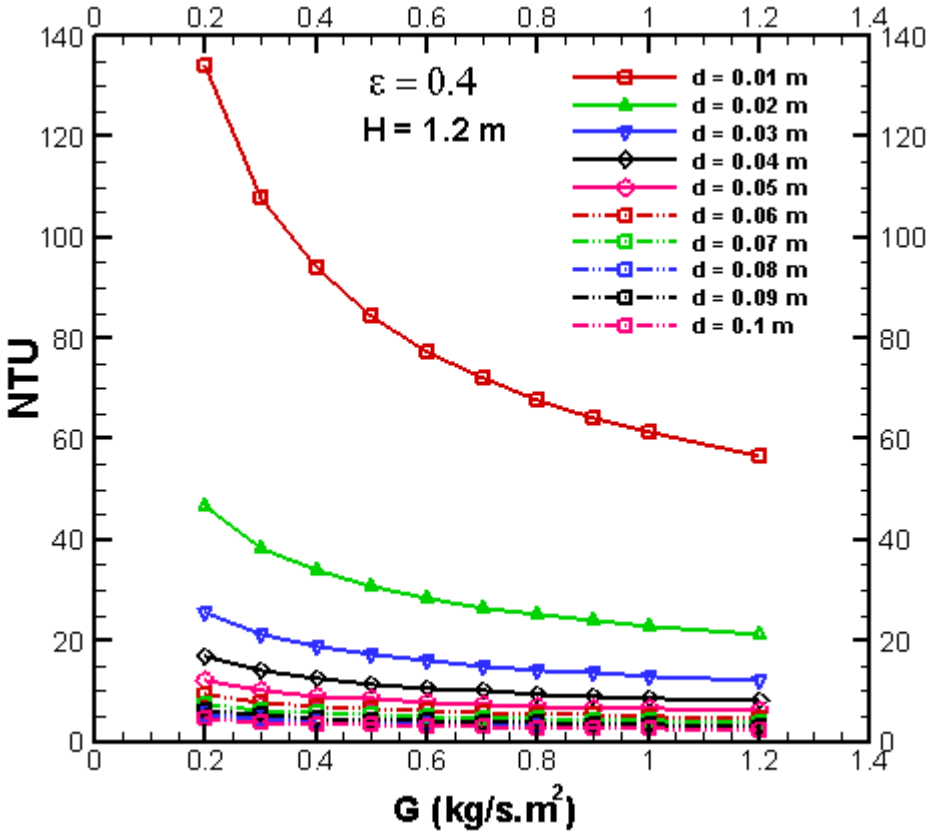

Fig.11-a: Variation of NTU with the mass velocity of HTF for various values of the solid particle diameter

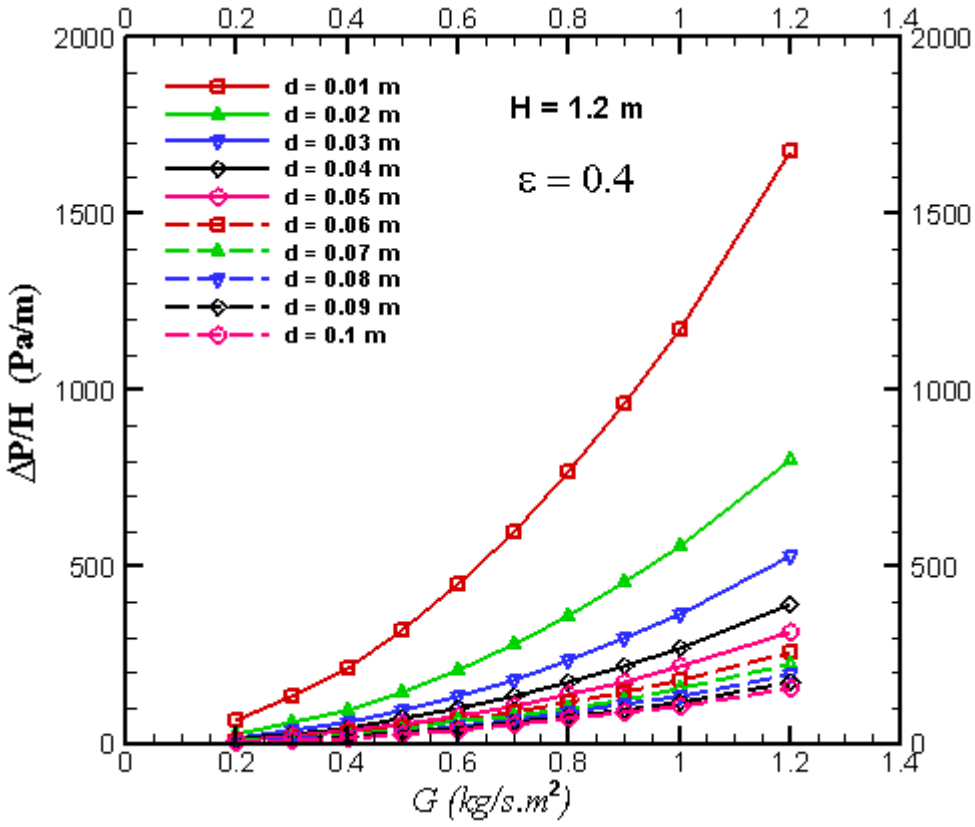

Fig.11-b: Variation of pressure drop with the mass velocity of HTF for various values of the solid particle diameter